Original research article

Arteriovenous fistula creation with VasQ™ device: A feasibility study to reveal hemodynamic implications

Michela Bozzetto[1] (iD), Luca Soliveri[2], Sofia Poloni[2] (iD),
Paolo Brambilla[3], Diego Curtò[4], Giuseppina Carmela Condemi[4],
Pietro Cefalì[5], Irene Spina[5], Alessandro Villa[6] (iD),
Anna Caroli[2] and Andrea Remuzzi[7] (iD)

Abstract

Background: Arteriovenous fistula (AVF) is the preferred vascular access (VA) for hemodialysis, but it is still affected by high non-maturation and early failure rates due to stenosis development. Increasing evidence suggests that the presence of turbulent-like flow may play a key role, therefore, to stabilize the flow in the venous segment, an external support device (VasQ™) has been designed. The aim of this study was to provide preliminary evidence of VasQ™ impact on AVF hemodynamics as compared to AVFs created with conventional surgery.

Methods: In this pilot single-center prospective randomized study six patients were enrolled, three in the VasQ group and three in the control group. Contrast-free magnetic resonance imaging (MRI) scans were acquired at 3 days, 3 months and 1 year after AVF surgery and were used to generate 3D patient-specific models. Computational fluid dynamic (CFD) simulations were performed using pimpleFoam, imposing patient-specific flow waveforms derived from ultrasound (US) examinations at the inlet of the proximal and distal artery, and a traction-free condition at the venous outflow. Morphologic and hemodynamic changes occurring over time were compared between VasQ and control AVFs.

Results: Our MRI protocol provided high-quality images suitable for reliable segmentation and reconstruction of patient-specific 3D models of AVFs at all three timepoints in four out of six patients. The VasQ™ device maintained the angle between the artery and the vein almost unchanged over time, with a more stable flow in the AVFs supported by the device. In contrast, one of the AVFs of the control group evolved to an extreme dilatation of the vein and highly disturbed flow, while the other developed a stenosis in the juxta-anastomotic region.

Conclusions: This study demonstrated the feasibility of characterizing the morphological and hemodynamic changes occurring over time in AVFs created using the VasQ™ device and provided preliminary evidence of the potential hemodynamic benefits of its use.

Keywords

Arteriovenous fistula, computational fluid dynamics, disturbed flow, external support device, longitudinal changes

Date received: 20 November 2021; accepted: 20 February 2022

[1]Department of Engineering and Applied Sciences, University of Bergamo, Italy
[2]Department of Biomedical Engineering - Istituto di Ricerche Farmacologiche Mario Negri IRCCS, Bergamo, Italy
[3]Diagnostic Radiology, Papa Giovanni XXIII Hospital, University of Milano-Bicocca, Milan, Italy
[4]Unit of Nephrology and Dialysis, ASST Ospedale Papa Giovanni XXIII, Bergamo, Italy
[5]Unit of Vascular Surgery, ASST Ospedale Papa Giovanni XXIII, Bergamo, Italy

[6]Department of Renal Medicine, Istituto di Ricerche Farmacologiche Mario Negri IRCCS, Bergamo, Italy
[7]Department of Management, Information and Production Engineering, University of Bergamo, Italy

Corresponding author:
Andrea Remuzzi, Department of Management, Information and Production Engineering, University of Bergamo, Via Marconi 5, Dalmine (BG), Italy.
Email: andrea.remuzzi@unibg.it

Introduction

Arteriovenous fistula (AVF) is the preferred vascular access (VA) for hemodialysis (HD) as it is associated with the highest patency and the lowest morbidity and mortality rate.[1,2] However, AVF is still affected by high non-maturation and early failure rates.[3,4] As a consequence, patients undergo frequent hospitalizations and emergency re-interventions, associated with a significant lowering of their quality of life and with a huge burden on healthcare systems.

The most common cause of AVF early-failure is vascular stenosis due to neointimal hyperplasia (NH).[5] Despite the exact mechanisms underlying stenosis development remaining unclear, computational fluid dynamic (CFD) simulations in idealized AVF models revealed that the locations where NH consistently develops are characterized by disturbed blood flow.[3] More recently, by investigating the patient-specific AVF hemodynamics, we also found that the venous segment may be characterized by turbulent-like flow, that could play a role in stenosis formation.[4,5]

Various strategies have been designed to regularize the hemodynamics in the venous segment of the AVF. Among them, the VasQ™ external support device (Laminate Medical Technologies, Israel) is a novel Nitinol implant, externally surrounding and supporting the vein and "hugging" the artery near the anastomosis without being in contact with the blood flow. The aim of using the VasQ™ is to maintain the optimal anastomotic angle, promoting a tapered transition of the venous outflow and favouring a more regular blood velocity pattern, as well as reinforcing the vulnerable perianastomotic vein against high pressure and wall tension. Recent studies demonstrated the device is safe, and reported improved functional patency for AVFs created using the VasQ™ as compared to AVFs created with conventional surgery.[6–11] However, the effect of the device on hemodynamic conditions and its role in regularizing the blood flow have yet to be adequately assessed. We have recently shown that coupling non-contrast enhanced magnetic resonance imaging (MRI) and high-resolution CFD provides a promising approach[12] to investigate AVF morphology and hemodynamics, possibly identifying critical hemodynamic conditions that may contribute to AVF remodelling after surgery.

The aim of the present study was then to explore the feasibility of characterizing the morphological and hemodynamic changes occurring over time in AVFs created using the VasQ™ device, also providing preliminary evidence of the differences with AVFs created using conventional end-to-side arteriovenous anastomosis.

Methods

Study population

This pilot single-center prospective randomized study was approved by the Local Ethics Committee (Reference number *NCT04141852*). Six patients referred for primary radio-cephalic AVFs at the Unit of Nephrology and Dialysis of the Papa Giovanni XXIII hospital (Bergamo, Italy) were enrolled in the study. Patients were considered for inclusion if they were between 18 and 75 years old and were suitable for a new AVF. Patients were excluded if they had prior VA in the same arm, contraindication to MRI examinations, known coagulation disorders and unusual anatomy or vessel dimensions, which could preclude VasQ™ implantation. All the patients enrolled in the study provided written informed consent. Since the age of the patients could importantly affect the feasibility of the MRI protocol, three age groups were identified (<45, 45–60, >60 years). Two patients per age group were enrolled in the study and randomly allocated on a 1:1 basis to AVF surgery using VasQ™ (VasQ group) or conventional AVF surgery (Control group). Patient allocation was performed at the Department of Bioengineering of the Istituto di Ricerche Farmacologiche Mario Negri IRCCS (Bergamo, Italy). All AVFs were created in the Department of Vascular Surgery of Papa Giovanni XXIII hospital (Bergamo, Italy) by the same vascular surgeon as first operator.

Magnetic resonance imaging acquisition and 3D AVF model generation

Contrast-free MRI scans were acquired at the Unit of Radiology of the Papa Giovanni XXIII hospital, at 3 days, 3 months and 1 year after AVF surgery. MRI sequences were obtained using a 1.5T scanner (GE, Optima 450w GEM) with a flexible 16-channel phased array medium coil and were cardiac gated using peripheral pulse gating. A three-plane scout sequence was first acquired to correctly localize the anastomosis. Then, 3D fast spin echo T1-weighted imaging was performed with variable flip angles using CUBE sequence, covering an arm region of approximately 5 cm above and 3 cm below the anastomosis, respectively. The 3D surface AVF models were reconstructed using the Vascular Modeling Toolkit (VMTK).[13] Straight cylindrical flow extensions of 5 diameters in lenght were added to ensure fully developed flow condition at the inlets. The discretization of the surface internal volume was obtained using FoamyHexMesh, which is part of OpenFOAM.[14] A grid convergence analysis[15] was performed and meshes of between 1000 k and 1300 k elements were generated accordingly, with dominant-hexahedral core cells, low orthogonality and predominant alignment to the vessel surface. Two thin boundary layers near the AVF wall were generated to catch the sharp velocity gradients denoting this area. The details of the grid convergence analysis and the mesh specific characteristics are reported in the Supplementary Tables 1–3.

Computational fluid dynamic simulation

Details on CFD simulation methodology are reported in our previous publication.[4] Briefly, CFD simulations were

Table 1. Demographic and clinical data of the four patients involved in the AVF geometric and hemodynamic characterisation. In V1 and V2 patients, the AVF was created using the VasQ device, while in the control patients (C1 and C2) it was created by conventional surgery.

	V1	V2	C1	C2
Gender	Male	Male	Male	Male
Age (years)	22	71	38	59
Diabetes	No	Yes	No	Yes
Hypertension	No	Yes	Yes	No
Cardiac disease	No	No	No	No
Dialysis treatment at AVF surgery time	Peritoneal dialysis	None	None	None
First dialysis after AVF surgery (days)	48	33	50	130
AVF status at 1 year	Patent	Patent	Patent	Patent (stenosis)

Abbreviations: AVF: arteriovenous fistula; V: VasQ; C: control.

performed using pimpleFoam, set with second-order spatial and time integration schemes. The timestep was adjusted automatically by the solver, resulting in an average duration of 0.04 ms. Patient-specific flow waveforms were derived from Ultrasound (US) examinations and imposed as boundary conditions at the inlet of the proximal and distal artery, while a traction-free condition was set at the venous outflow. Three complete cardiac cycles were solved and only the third one was used for post-processing in order to avoid start-up transients. Blood was modelled as patient-specific, non-Newtonian fluid using the Bird-Carreau rheological model, assuming a blood density of 1.05 g/cm^3 and using patient-specific hematocrit and total serum proteins. The CFD simulations were performed under the rigid wall assumption.

Hemodynamic and morphological changes' analysis

The post-processing of CFD results was performed using Paraview.[16] The velocity phenotype was qualitatively characterized using the velocity 3D streamlines and velocity waveforms at selected equally spaced points along the vessel centerline. The Time Averaged Wall Shear Stress (TAWSS) along a cardiac cycle of period T was calculated as

$$TAWSS = \frac{1}{T} \int_0^T |\tau_\omega| \, dt$$

Furthermore, the Oscillatory Shear Index (OSI), that quantifies the degree of deviation of the WSS from its average direction,[17] was calculated as

$$OSI = \frac{1}{2} \left(1 - \frac{\left| \int_0^T \tau_\omega dt \right|}{\int_0^T |\tau_\omega| \, dt} \right)$$

To characterize AVF morphological changes over time, a rigid co-registration of the 3D models generated at the different timepoints was performed using the iterative closest point (ICP) registration algorithm of VMTK. Subsequently, vascular lumen cross-sectional areas (CSAs) along the venous centerline were extracted from the center of the anastomosis to 2 cm along the distal vein (i.e., over the vessel segment supported by the VasQ^{TM} device) every 0.1 mm. Moreover, for every 3D model we extracted the angle between the artery and the vein (see Supplementary Figure 1). To characterize the hemodynamic changes over time and the differences between the VasQ and control AVFs, the TAWSS and the OSI were extracted and averaged for each slice previously isolated. To investigate the differences in CSA, OSI, and TAWSS between VasQ and control AVFs, a Wilcoxon test was performed using R version 4.2.[18] Statistical significance was set at $p < 0.05$.

Results

Five out of six patients underwent AVF MRI scans at all three timepoints, while one patient in the VasQ group underwent a single MRI scan at 3 days after surgery and then refused to repeat MRI due to claustrophobia. Our MRI protocol provided high-quality images suitable for reliable segmentation and reconstruction of patient-specific AVF 3D models at all three time points in four out of six patients. Beyond the VasQ patient with a single MRI scan, a patient of the control group aged > 60 years had all MRI scans denoted by blurring, most probably due to his involuntary movement during acquisition, and thus not usable for reliable processing. Clinical and demographic data of the four patients included in the final analysis (2 VasQ-V1 and V2, and 2 control ones-C1 and C2) are reported in Table 1. All the AVFs were deemed clinically matured and were successfully cannulated with two needles within 3 months after surgery.

The 3D patient-specific AVF models and pertinent blood flow rates at different time points are reported in Figure 1. They look very heterogeneous, both immediately
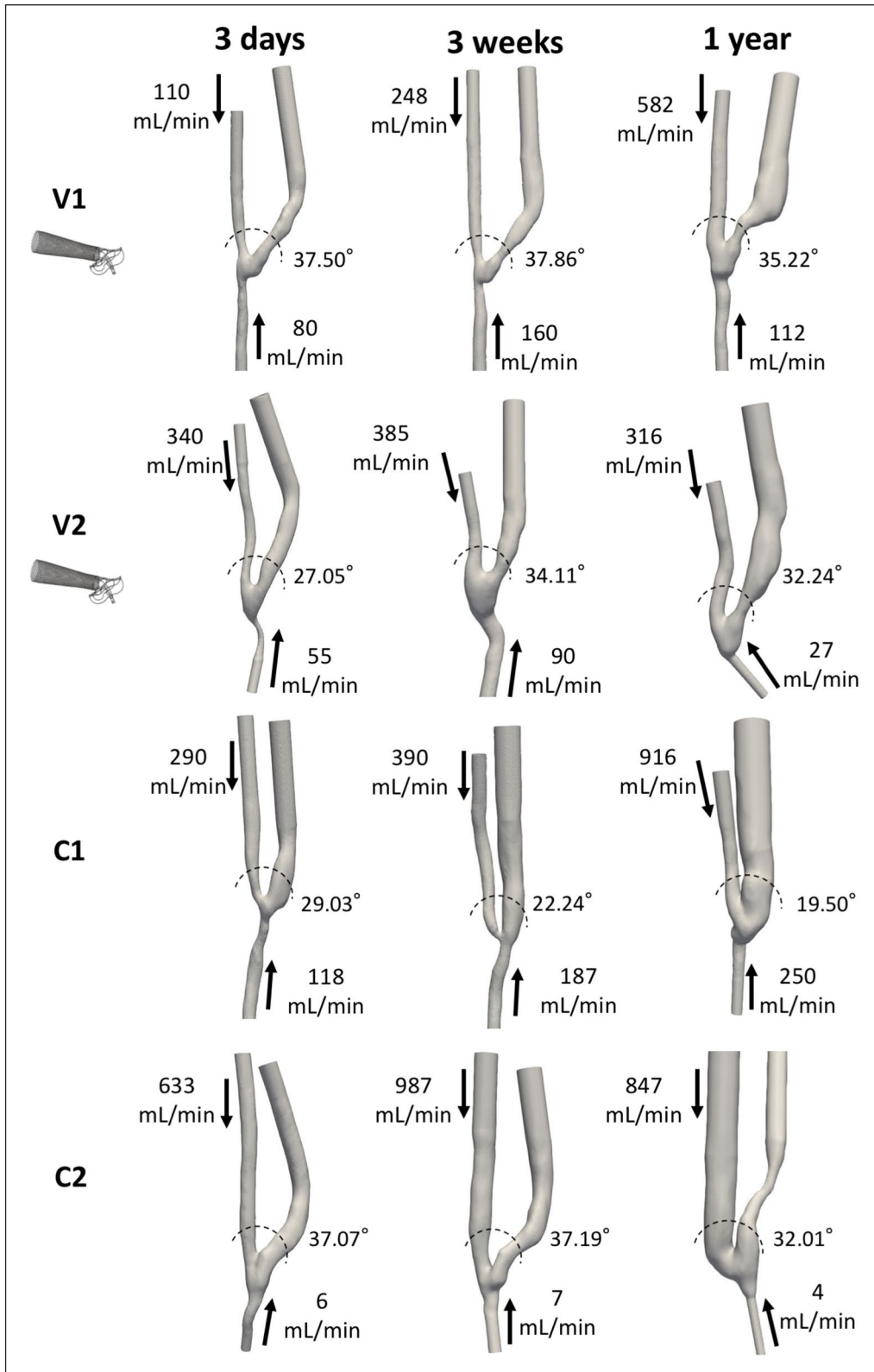
Figure 1. Three dimensional geometrical models and blood flow rates of the two AVFs created using the VasQ device (V1 and V2) and the two control AVFs created by conventional surgery (C1 and C2), at 3 days, 3 weeks and 1 year after surgery. Arrows indicate the main direction of blood flow. The amplitude of the angle between the proximal artery and the vein is also shown for each model.
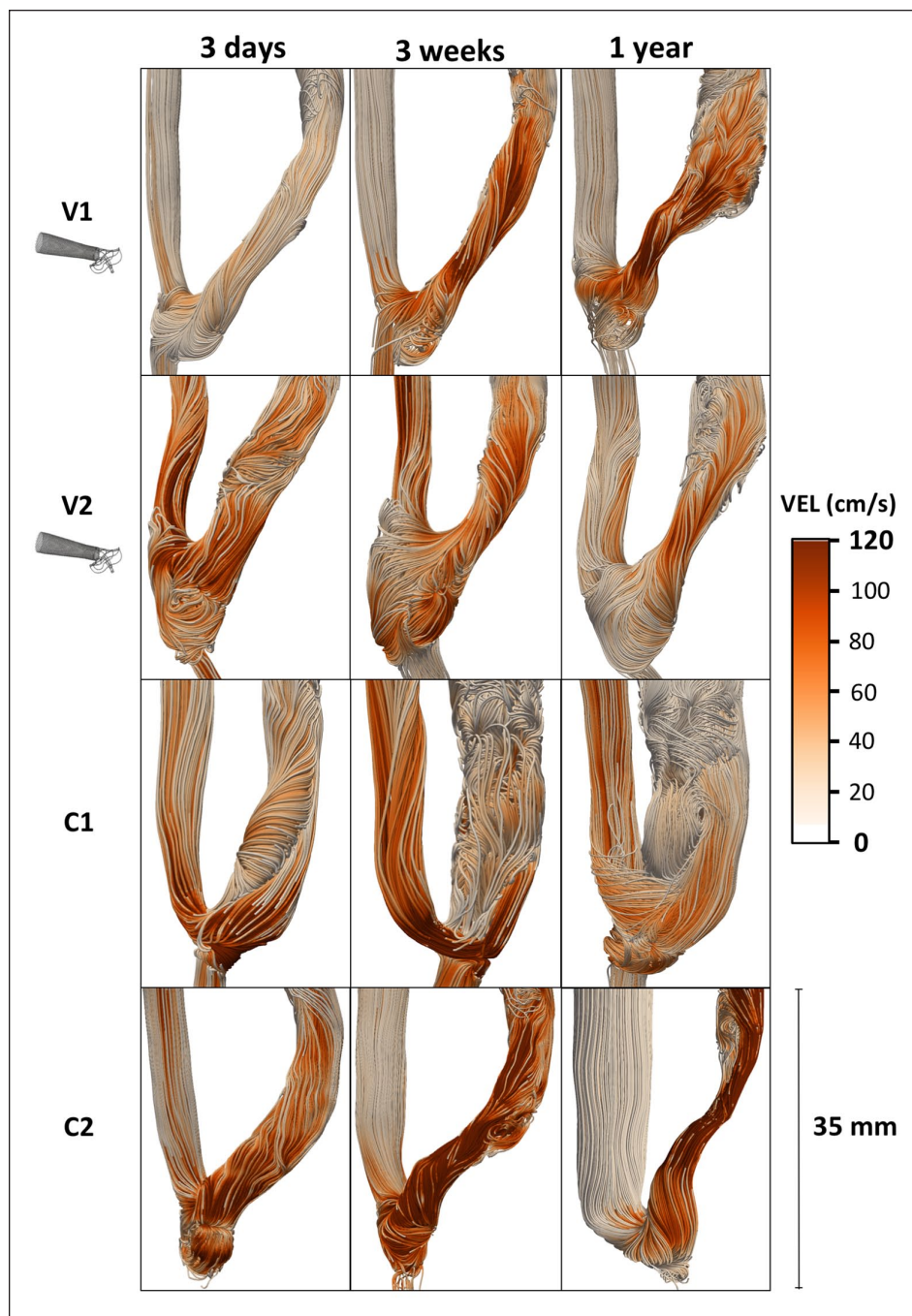
Figure 2. Velocity streamlines at the systolic peak in the four AVFs under study, two ones created using the VasQ device - V1 and V2, and two control ones created by conventional surgery - C1 and C2, at 3 days, 3 weeks, and 1 year after surgery.

after surgery and in terms of evolution over time. In the VasQ group, patient V1 showed a constant increase in the blood flow rate, which doubled at 3 weeks and was five-fold at 1 year after surgery, while in patient V2 the blood flow rate remained almost unchanged over time. In the control group, patient C1 showed a constant increase in the blood flow rate up to 1 year, while C2 showed a rapid increase up to 3 weeks followed by a decrease in blood flow, that remained adequate for HD treatment up to 1 year after surgery. As for the morphological changes, the AVF

geometry of the two patients with VasQ™ was similar between 3 days and 3 weeks after surgery, while showing a dilatation at 1 year in the vein right after the VasQ™ device. In contrast, AVF geometry significantly changed between 3 days and 3 weeks in both patients of the control group, with C1 patient showing a significant dilatation of the vein and C2 a stenosis in the same segment.

Hemodynamic changes reflect the morphological evolution, especially in the control group. Figure 2 shows the blood flow velocity streamlines at the systolic peak.

Immediately after surgery, all the patients showed a laminar flow with well-aligned or helical streamlines in the vein. In the patients with the VasQ™ device the flow was laminar up to 3 weeks and then became unsteady in the distal segment of the vein at 1 year after AVF surgery. The two control patients showed completely different blood flow velocity evolution over time: patient C1 showed a highly disturbed flow since 3 weeks after surgery; on the contrary, the stenosis of patient C2 resulted in the stabilization of the streamlines in the narrowing areas, immediately followed by unsteady flow in the vein segment distal to it.

The velocity traces extracted along the models' centreline, shown in Figure 3, confirm and complete the previous results. In all the patients the velocity profile is laminar in the proximal artery and becomes unstable at the anastomosis. In patients V1 and V2 the traces of the segment closed to the anastomosis and supported by the device (locations 5 and 6) tend to regularize over time, with an evident damping of the oscillations and a retrieve of the pulsatile waveform. With increasing distance from the anastomosis (locations 7–9) the velocity profile is denoted by high frequent oscillations, which tend to damp over time. On the contrary, patient C1 exhibits high frequency fluctuations of the velocity waveforms for all follow-up time points after surgery, while the stenosis in C2 causes the complete regularization of the velocity profiles at 1 year after surgery.

The surface maps of TAWSS and OSI parameters are reported in Figure 4, allowing to further characterize the blood flow field. Patients with VasQ™ were characterized by very low OSI in the area of the vein supported by the device and higher values along the distal vein with venous regions of high OSI becoming wider over time. Most of the regions with high OSI were characterized by low TAWSS. In the control group the scenario was more heterogenous. Patient C1 showed large areas of high OSI at 3 weeks, slightly decreasing in size at 1 year, with TAWSS instead decreasing over time, especially in the most dilated segments. Patient C2 presented very low OSI in the stenotic areas at 3 weeks and 1 year after surgery, and higher OSI in the distal vein, while the TAWSS in the stenotic areas increased over time.

The boxplots reported in Figure 5 show the CSAs changes that occurred in the first 2 cm of vein (a) and the changes in TAWSS and OSI over time (b), in VasQ and control patients. Three weeks after surgery the CSAs of the vein segment contained in the VasQ™ were unchanged, while control patients showed a predominant dilatation and only small areas with stenosis development. The dilatation of the vein and the narrowing in control patients boosted during the time period between 3 weeks and 1 year, while VasQ segments remained mostly stable. Regarding the hemodynamic indexes, at the time of surgery, VasQ patients showed significantly higher OSI as compared with the controls. Oscillatory shear index remained almost unchanged in the VasQ patients during the first 3 weeks after surgery, while in controls it increased significantly. Moreover, VasQ patients showed lower TAWSS values than the controls at 3 days and 3 weeks after surgery. At 1 year, OSI was almost unchanged in VasQ patients, while it reduced in controls. Time averaged wall shear stress remained unchanged in the VasQ group, while increased over time in the control group.

Discussion

This study demonstrated the feasibility of adopting a MRI-based CFD analysis to characterize the morphological and hemodynamic changes occurring over time in AVFs created using the VasQ™ device and provided some insights into the mechanism of vascular remodeling observed to date. Four out of the six enrolled patients successfully completed all the steps of the MRI-to-CFD pipeline, demonstrating the feasibility of the methodology. The two patients that did not complete the follow-up scans successfully were due to factors beyond the control of the investigators. Data collected from four patients that completed the study suggest a potential benefit of the VasQ™ device in maintaining a more stable morphology and hemodynamic profile with time.

The longitudinal morphological and hemodynamic characterisation of both VasQ and control AVFs is an achievement in itself. Indeed, only two MRI-based studies in the literature included longitudinal data on AVF remodelling in patients.[19,20] This study is the first to generate a randomized, prospective comparison of two different AVF strategies and expand the discussion on addressing key factors of negative remodelling. Our study also highlighted a potential exclusion criterion for future MRI-based studies. The patient who had poor quality MR images at all time points that did not allow for reliable 3D model reconstruction and CFD simulation, was part of the most advanced age group. The MRI artefacts were due to tremors that were not caused by a known pathology, and likely resulted only from musculoskeletal pain and consequent difficulty in staying still inside the MR machine. This suggests that advanced age or certain underlying conditions may affect the feasibility of such investigation.

Moreover, the present investigation allowed highlighting differences in CSAs and hemodynamic indices in VasQ as compared to control AVFs, importantly extending the results of the studies on the VasQ™ device that have been published in the literature so far. The first experience with VasQ™ was reported by Chemla et al.,[6] who implanted VasQ™ devices in twenty patients undergoing brachiocephalic AVF surgery and confirmed safety and high unassisted maturation and patency rates. Then, the studies of Shahverdyan et al.[8] and Benedetto et al.[11] further demonstrated the safety and essentially confirmed the promising results in terms of primary and functional patency of VasQ
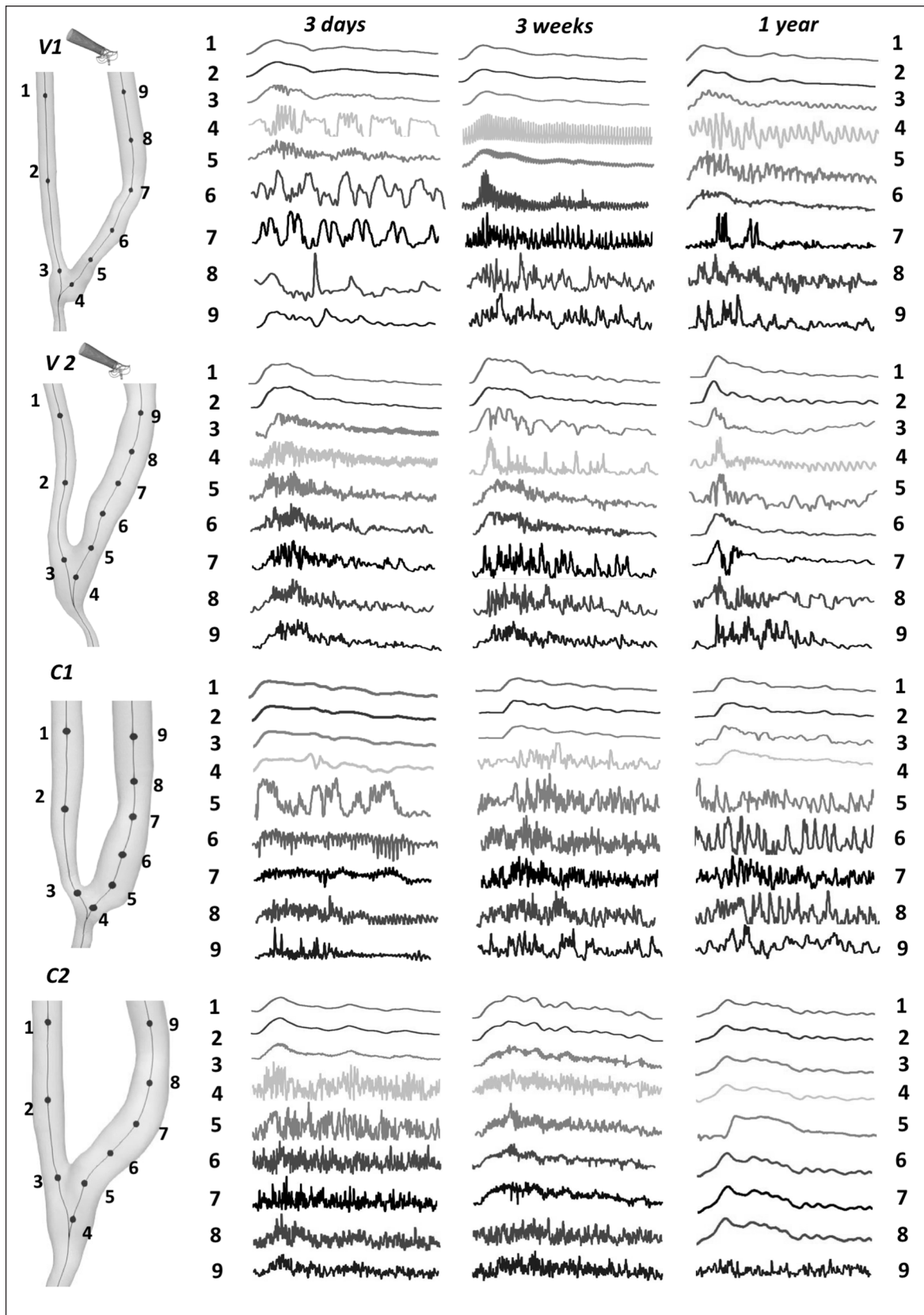
Figure 3. Velocity-time traces, normalized by their respective cycle averages, at nine selected feature points along the centerline in the four AVFs under study, two ones created using the VasQ™ device - V1 and V2, and two control ones created by conventional surgery - C1 and C2, at 3 days, 3 weeks, and 1 year after surgery.
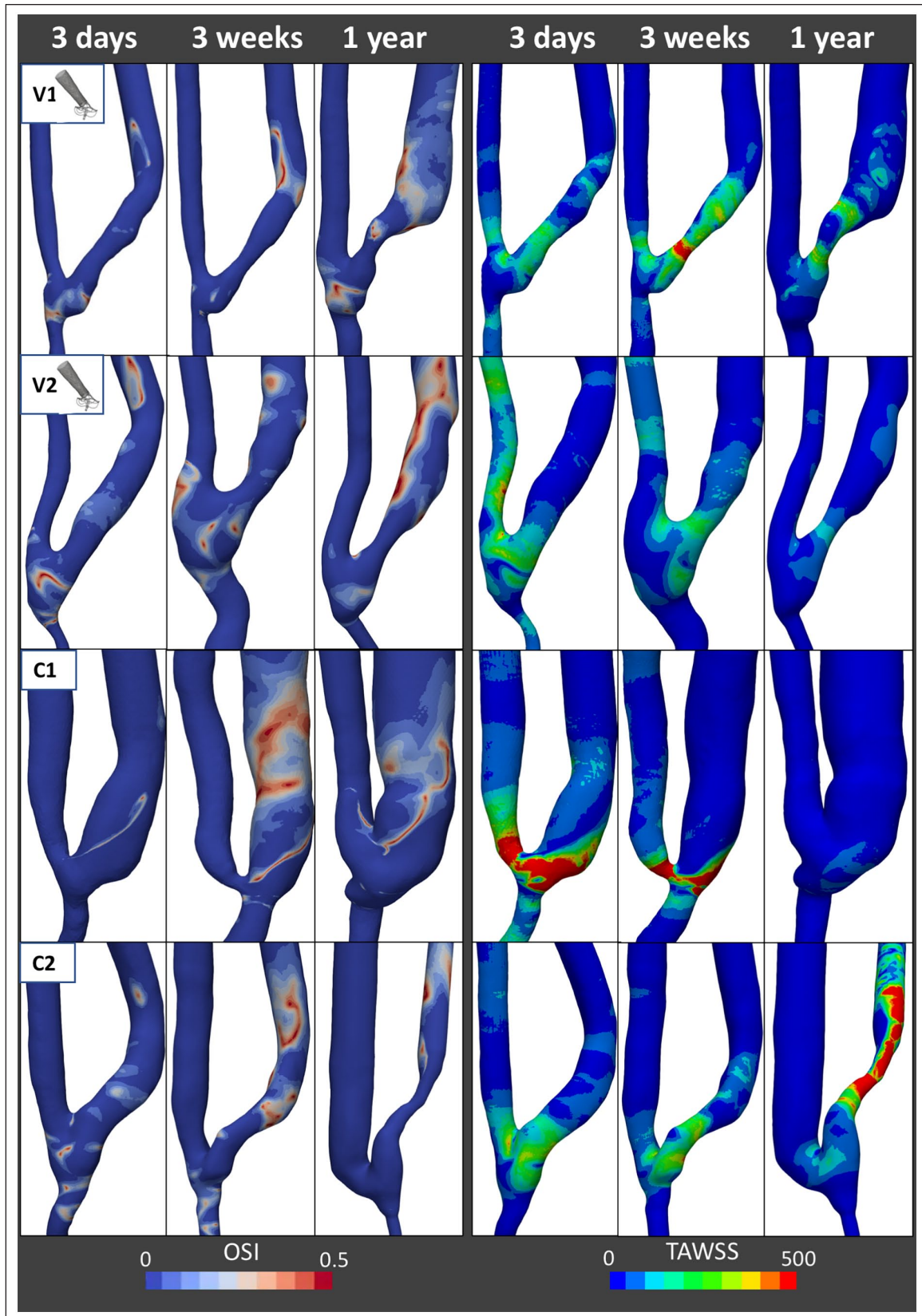
Figure 4. Oscillatory shear index (OSI) and time averaged wall shear stress (TAWSS) surface maps of the four AVFs under study, two ones created using the VasQ™ device - V1 and V2, and two control ones created by conventional surgery - C1 and C2, at 3 days, 3 weeks and 1 year after surgery.
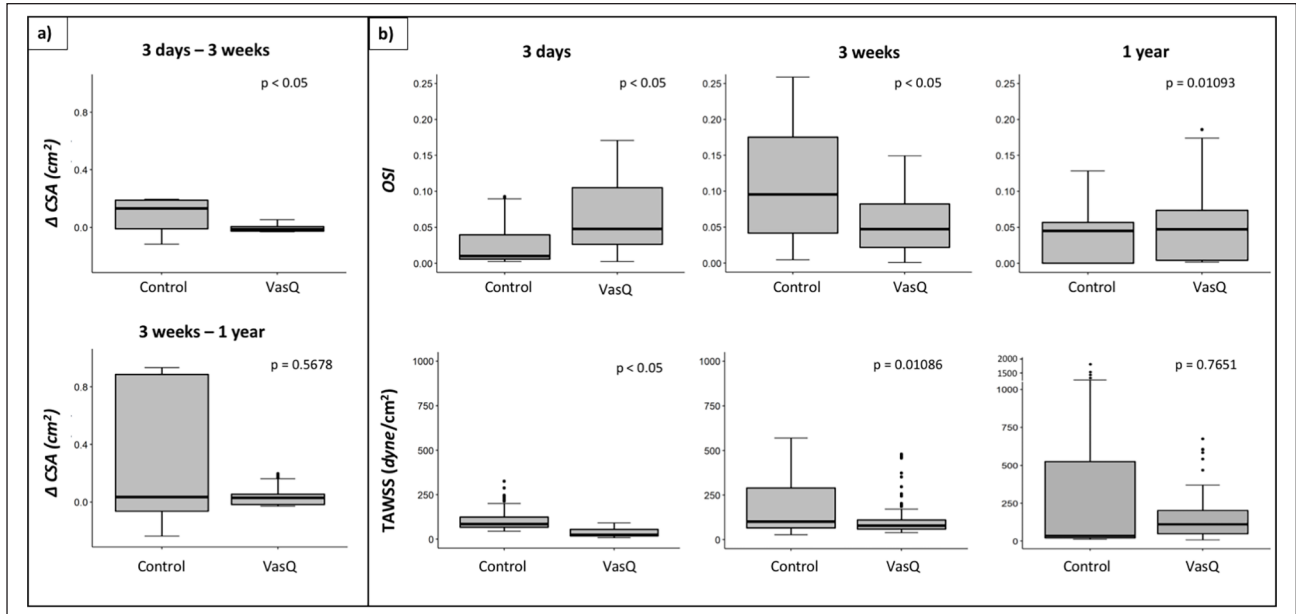
Figure 5. Distribution of (a) the variation of cross sectional areas (CSAs) between different timepoints; (b) Oscillatory shear index (OSI); and time averaged wall shear stress (TAWSS) by AVF group (VasQ vs. control) at the three study timepoints. The thick line denotes the median, the box goes from the first to the third quartile, and the whiskers show the minimum and maximum data.

AVFs as compared to the standard of care of their clinical centers. However, both studies were limited by their retrospective nature. The only prospective trial on VasQ AVFs was conducted by Karydis et al.,[7] who found a significantly higher functional patency (2-needle cannulation of patent AVFs for two-thirds or more of all dialysis runs over a 1 month period) in AVFs created using VasQ™ device as compared to control AVFs (100% vs. 56%) at 6 months, and related this finding to the higher vein luminal diameters observed in VasQ AVFs at 3 and 6 months after surgery, which may have favored successful cannulation. The study also reported a significantly lower rate of stenosis ≥50% of the luminal diameter for the VasQ group as compared to the control. However, the Authors did not observe significant differences between the study groups in the functional patency rate at 6 months albeit the VasQ group was higher. Only the recent investigation by Palumbo et al.,[21] who concluded that VasQ™ may provide a benefit in preventing the overload of the left ventricle by reducing the altered high cardiac output, can be seen as a first step into a better understanding of hemodynamic modifications related to VasQ™ devices in the cardiovascular system. However, none of these studies could confirm if the proposed mechanism related to VasQ™ implantation was driving the clinical benefits that were being reported.

This is the first study providing preliminary evidence of a more stable morphologic and hemodynamic evolution of VasQ AVFs as compared with control ones. Indeed, the VasQ™ device created a tapered transition of flow and made the angle between the artery and the vein remaining almost unchanged over time. The blood flow volume

gradually increased in patient V1 and remained constant after the initial sudden increase in patient V2 (see Figure 1). At 1 year both AVFs showed a similar pattern of regular flow in the peri-anastomic area, with blood velocity mainly parallel to the vessel wall. In these AVFs vessel dilatation and unstable flow developed in the venous segment more distally, but this flow condition, characterized by low WSS, is not likely to affect AVF patency. It is also possible that in these distal parts of the AVFs after the VasQ™, low WSS, and high OSI may be responsible for vessel dilation. However, longer follow-up data would be needed to elucidate AVF evolution after 1 year. On the contrary, vessel adaptation after conventional AVF surgery was heterogeneous in nature and highlights the unpredictable nature of AVF maturation. In one case, extreme dilatation of the vein was observed with high blood flow rates. In the other, the development of a stenosis occurred in the juxta-anastomotic region. Indeed, despite the blood flow rate in both C1 and C2 AVFs at 1 year after surgery being completely adequate for HD treatment (see Figure 1), patient C1 may evolve to a high-flow AVF and consequent risk of cardiac overload.[22,23] On the contrary, in patient C2 the concomitant significant dilatation of the arterial segment may have partially compensated the vein stenosis and contributed to the adequate flow so far. However, a decrease in blood flow volume requiring strict surveillance is expected to occur with further progression of the stenosis and AVF failure.

The reasons why the two control AVFs evolved to such different scenarios remain unclear, mostly because the relationship between the hemodynamic conditions and the

AVF remodelling still needs to be fully elucidated. Specifically, the mechanism leading to stenosis development is still poorly understood, and further understanding may improve the prevention of AVF dysfunction. Disturbed flow has been considered to play an important role in stenosis formation since a long time, but no hemodynamic parameters have been found to unequivocally correlate with stenosis formation in AVF yet. However, taking a step back in the cause-effect relation, some noteworthy studies have been conducted to understand the role of AVF geometry in triggering disturbed flow. From our group, Ene-Iordache et al.[24] investigated the influence of the anastomosis angle on the pattern of disturbed flow in idealized models of wrist side-to-end radial-cephalic AVF, showing that at 30° and 40° the areas of disturbed flow were smaller as compared to greater angles. Clinical observations of Sadaghianloo et al.[25] reported increased reinterventions in radial-cephalic AVFs with anastomotic angles of less than 30°. Therefore, the possibility to obtain an acute and fixed angle with the VasQ™ device seems to be an important feature to improve AVF outcome and an interesting factor to be investigated on a larger number of patients. This is the first clinical study that demonstrated that the tapered configuration is retained over the long-term after AVF maturation, reducing locally the disturbed flow areas. Our results suggest that keeping a constant acute angle with the VasQ™ device and a tapered geometry of the out-flow vein segment in AVF are important features to improve AVF outcome and worth investigating on a larger number of patients.

The main limitation of the present study is the small sample size that allowed only preliminary observations on the effect of VasQ™. However, we studied only two patients per group to assess the feasibility of comparing VasQ and control AVFs in a prospective study and in the long term. Moreover, the study included only side-to-end AVFs but this is due to the fact that VasQ device was designed to create only this type of anastomosis.

Another limit of our investigation is that CFD simulations did not account for the effect of the vessel wall compliance. This issue could be addressed in future studies by conducting fluid–structure interaction (FSI) simulations. McGah et al.[26] determined that rigid-wall hemodynamic simulations can predict blood hemodynamics within the same order of accuracy of the FSI equivalent simulations, but how VasQ™ device affects stresses in the vascular wall will be an interesting future development. Despite the limitations, this study demonstrated the feasibility of characterizing the morphological and hemodynamic changes occurring over time in AVFs created using the VasQ™ device and provided preliminary evidence of the potential benefits of these devices to regularize blood flow field in time. Future clinical investigations with higher number of patients are required to confirm current preliminary findings, fully investigate the role of VasQ™ device in flow regularization and elucidate its potential in preventing stenosis development and AVF failure.

ORCID iDs

Michela Bozzetto https://orcid.org/0000-0002-2045-5550
Sofia Poloni https://orcid.org/0000-0002-9402-9925
Alessandro Villa https://orcid.org/0000-0001-5556-5701
Andrea Remuzzi https://orcid.org/0000-0002-4301-8927

Supplemental material

Supplemental material for this article is available online.

References

1. Drew DA, Lok CE, Cohen JT, et al. Vascular access choice in incident hemodialysis patients: a decision analysis. *J Am Soc Nephrol* 2015; 26(1): 183–191.
2. Böhlke M, Uliano G and Barcellos FC. Hemodialysis catheter-related infection: prophylaxis, diagnosis and treatment. *J Vasc Access* 2015; 16(5): 347–355.
3. Ene-Iordache B and Remuzzi A. Disturbed flow in radial-cephalic arteriovenous fistulae for haemodialysis: low and oscillating shear stress locates the sites of stenosis. *Nephrol Dial Transplant*. 2012; 27(1): 358–368.
4. Bozzetto M, Ene-Iordache B and Remuzzi A. Transitional flow in the venous side of patient-specific arteriovenous fistulae for hemodialysis. *Ann Biomed Eng*. 2016; 44: 2388–2401.
5. Remuzzi A and Bozzetto M. Biological and physical factors involved in the maturation of arteriovenous fistula for hemodialysis. *Cardiovasc Eng Technol* 2017; 8(3): 273–279.
6. Chemla E, Velazquez CC, D'Abate F, et al. Arteriovenous fistula construction with the VasQ external support device: a pilot study. *J Vasc Access* 2016; 17(3): 243–248.
7. Karydis N, Bevis P, Beckitt T, et al. An implanted blood vessel support device for arteriovenous fistulas: a randomized controlled trial. *Am J Kidney Dis* 2020; 75(1): 45–53.

8. Shahverdyan R, Meyer T and Matoussevitch V. Patency and functionality of radiocephalic arteriovenous fistulas with an external support device (VasQ™): real-world single-center experience. *J Vasc Access* 2021; 22(2): 166–172.

9. Shahverdyan R, Tabbi P and Mestres G. Multicenter European real-world utilization of vasq™ anastomotic external support device for arteriovenous fistulae. *J Vasc Surg* 2022; 75(1): 248–254.

10. Leonardi G, Campagna M, Pellicanò V, et al. Implanted blood vessel external support device (VasQ™) for creation of hemodialysis arteriovenous fistula: a single-center experience. *J Vasc Access*. 2020; 22(4): 658–665.

11. Benedetto F, Spinelli D, Derone G, et al. Initial single-center experience with a new external support device for the creation of the forearm native arteriovenous fistula for hemodialysis. *J Vasc Access*. Epub ahead of print 16 March, 2021. DOI: 10.1177/11297298211002570.

12. Bozzetto M, Brambilla P, Rota S, et al. Toward longitudinal studies of hemodynamically induced vessel wall remodeling. *Int J Artif Organs* 2018; 41(11): 714–722.

13. Antiga L, Piccinelli M, Botti L, et al. An image-based modeling framework for patient-specific computational hemodynamics. *Med Biol Eng Comput* 2008; 46(11): 1097–1112.

14. OpenFoam T. The OpenFOAM Foundation. http://www.openfoam.org (2014, accessed 18 November 2021)

15. Procedure for estimation and reporting of uncertainty due to discretization in CFD applications. *J Fluids Eng* 2008; 130(7): 078001.

16. ParaView. Unleash the power of ParaView, http://www.paraview.org

17. Ku DN, Giddens DP, Zarins CK, et al. Pulsatile flow and atherosclerosis in the human carotid bifurcation. Positive correlation between plaque location and low oscillating shear stress. *Arteriosclerosis* 1985; 5(3): 293–302.

18. R: The R project for statistical computing. https://www.r-project.org/ (2021, accessed 22 July 2021).

19. Sigovan M, Rayz V, Gasper W, et al. Vascular remodeling in autogenous arterio-venous fistulas by MRI and CFD. *Ann Biomed Eng* 2013; 41(4): 657–668.

20. He Y, Terry CM, Nguyen C, et al. Serial analysis of lumen geometry and hemodynamics in human arteriovenous fistula for hemodialysis using magnetic resonance imaging and computational fluid dynamics. *J Biomech* 2013; 46(1): 165–169.

21. Palumbo R, Dominijanni S, Centi A, et al. Hemodynamic impact of VASQ device in vascular access creation. *J Vasc Access* 2020; 23(1): 105–108.

22. Badero OJ, Salifu MO, Wasse H, et al. Frequency of swing-segment stenosis in referred dialysis patients with angiographically documented lesions. *Am J Kidney Dis* 2008; 51(1): 93–98.

23. Basile C, Lomonte C, Vernaglione L, et al. The relationship between the flow of arteriovenous fistula and cardiac output in haemodialysis patients. *Nephrol Dial Transplant* 2008; 23(1): 282–287.

24. Ene-Iordache B, Cattaneo L, Dubini G, et al. Effect of anastomosis angle on the localization of disturbed flow in 'side-to-end' fistulae for haemodialysis access. *Nephrology Dialysis Transplantation* 2013; 28(4): 997–1005.

25. Sadaghianloo N, Jean-Baptiste E, Rajhi K, et al. Increased reintervention in radial-cephalic arteriovenous fistulas with anastomotic angles of less than 30 degrees. *Journal of Vascular Surgery* 2015; 62(6): 1583–1589.

26. McGah PM, Leotta DF, Beach KW, et al. Effects of wall distensibility in hemodynamic simulations of an arteriovenous fistula. *Biomech Model Mechanobiol* 2014; 13(3): 679–695.